3D Analysis of Variation in Alveolar Cleft Defect Shape and Size

BY

NORA M. BAKHSH

B.D.S, King AbdulAziz University 2012

THESIS

Submitted as partial fulfillment of the requirements for

The Master of Science in Oral Sciences in the Graduate

College of the University of Illinois at Chicago, 2020

Chicago, Illinois

Defense Committee:

Dr. Christina Nicholas, Chair and Advisor

Dr. Veerasathpurush Allareddy

Dr. Lina Moreno-Uribe, University of Iowa

This work is dedicated to my little family, my husband who I couldn’t have done this without and my two girls who bring joy to my life every day.

ACKNOWLEDGMENTS

Kareem Abed: No wards can thank you enough! I couldn't have made it through whole journey without you, you have been there for me every step of the way and I have not been able to do it without your support and love,

Dr. Christina Nicholas: Thank you for being a great advisor! Thank you for all your help and support, including calming me down time every time I start to stress out. I have learnt a lot from you and you have made this an easier and a more productive experience.

Dr. Veerasathpurush Allareddy: Thank you for all your help and feedback. Thank you for all your work for this department, and thank you for all your support.

Dr. Lina Moreno-Uribe: Thank you for giving us the subjects for this project, and thank you for all your help, in-put and feedback and support.

Yena Jun: My project buddy! Thank you for your support and feedback through out! I am glad that we had to do this together. It wouldn't have been the same without you!

NMB

Table of Contents

LIST OF TABLES

LIST OF FIGURES

LIST OF FIGURES (continued)

LIST OF ABBREVIATIONS

ALP	Alkaline Phosphatase
BMP	Bone Morphogenetic Protein
B-TCP	B-Tricalcium Phosphate
CAE	Computer-Aided Engineering
CDC	Centers for Disease Control and Prevention
CL/P	Cleft Lip With Or Without Cleft Palate
DPP	Deproteinized Bovine Bone
GPP	Gingivoperiosteoplasty
GTR	Guided Tissue Regeneration
HMSCS	Available Human Mesenchymal Stem Cells
NAM	Naso-Alveolar Molding
PSIO	Pre-Surgical Infant Orthopedics
RH-BMP2	Recombinant Human Bone Morphogenetic Protein-2
SEM	Scanning Electron Microscopy

SUMMARY

An alveolar cleft is a cleft in the primary palate located anterior to the incisive foramen (Bajaj et al, 2003). Currently, secondary bone grafting with cancellous bone from the iliac crest is the golden standard for treatment of alveolar clefts (Bajaj et al, 2003). However, some disadvantages have been reported. Revington et al. (2008) studied 235 grafted sites and reported a failure rate of 24%. Donor site morbidity is another downside of autogenous bone grafting. Brudnicki et al, (2018) studied donor site morbidity and reported that 93% of the patients reported donor site pain equal to or exceeding the recipient site, while 92% reported gait disturbances following surgery. To overcome the current drawbacks of treatment methods, 3D printed tissue engineered scaffolds are being investigated (e.g., Berger et al, 2015). With this new treatment potential, preoperative understanding of the alveolar cleft architecture, size and volume is needed to provide better understanding of scaffolds biomechanics, and opens a new potential for pre-made alveolar grafts.

This current study investigated the variability in shape and volume of 32 unilateral and bilateral cleft patients. The sample consists of 32 unilateral or bilateral cleft patients who are undergoing a secondary alveolar graft. 3D Slicer software (Pieper et al., 2004) was used to construct 3D models of the cleft defects from CBCTs that were taken prior to the graft. After that, shape geometric morphometric analyses were performed, followed by statistical analyses (in the statistical program R).

SUMMARY (CONTINUED)

In regard to size, the average volume for alveolar defects was 783.9 mm^3, while the average height and width (at the nasal floor) were 12.17 mm and 11.62 mm, respectively. In addition, the unilateral alveolar defects were on average larger than bilateral defects with statistically significant differences in volume and height, and width at the nasal floor approaching significance.

The shape cluster analysis indicated that a 2-cluster model best fit the shape variation data. These two clusters appear to describe clefts that are either relatively wide (mediolaterally) or in contrast relatively tall (supero-inferiorly). However, the Bayesian Information Criterion (BIC) was interpreted as indicating potential evidence to support a 5-cluster model. As a result, a 5-cluster model was considered as an alternative which might better represent the wide range of variability. Broadly speaking, the five groups were: 1) tall, rectangular with similar widths superiorly and inferiorly as well as anteriorly and posteriorly; 2) relatively square (anteriorly); 3) wedge-shaped (wider superiorly) with a wider surface posteriorly than anteriorly; 4) wedge-shaped (wider superiorly) with similar anterior-posterior widths; 5) wide, rectangular with a much larger medio-lateral breadth width than supero-inferior height.

In conclusion, we show great variability in alveolar cleft defect size and shape. However, most clefts are roughly square, rectangular, or a wedge with a wider superior (nasal floor) surface. Further research with a larger sample size and un-operated cleft defects is needed to confirm the variability captured in our 5-cluster model and to assess the relative frequency of different cleft defect sizes and shapes.

I. INTRODUCTION

I.1. Background

An alveolar cleft is a gap in the alveolar bone as the result of abnormal primary palate formation and it is one of the most common craniofacial birth defects alongside other manifestations of cleft lip and cleft palate. According to Bajaj and colleagues (2003), secondary bone grafting with autogenous cancellous bone is the gold standard nowadays for treatment of alveolar clefts. However, because of the disadvantages of this method including high failure rates and donor site morbidity, new treatment modalities are being studied (e.g., Revington et al., 2008; Berger et al., 2015). The ideal would be to eliminate the need for bone grafting. Thus, using a 3D printed tissue engineered scaffold as a grafting material is being investigated as an alternative treatment method (Berger et al., 2015; Palhazi et al., 2015).

With this new treatment potential, an understanding of alveolar cleft architecture, size, shape and volume is needed for two key reasons. Firstly, biomaterials chosen for bioprinted grafts will need to be sufficient to handle the biomechanical strain of the cleft (which may differ by cleft size) and allow for propagation of cells across different volumes of printed tissue. Secondly, while bioprinted scaffolds, if developed, are likely to represent an advancement in personalized medicine in developed countries, custom grafts will not be practical in all treatment settings. Thus, understanding the range of variability in size and shape may allow for the development of prefabricated, standardized grafts for use in settings where taking a CT scan is not possible. However, current classification systems for clefts focus on location (Shah et al. 2011) and studies investigating alveolar cleft morphology and volume are lacking.

I.2. Aim

The objectives of this study were to investigate the variability in shape and volume of alveolar clefts and determine if alveolar clefts have common forms. This study further compares unilateral and bilateral cleft volumes and sizes.

I.3. Null hypotheses

- Alveolar cleft defects cannot be grouped into meaningful categories based upon 3D shape
- There is no difference in alveolar cleft defect volume between unilateral and bilateral clefts.
- There is no difference in alveolar cleft defect height between unilateral and bilateral clefts.
- There is no difference in alveolar cleft defect width at the nasal floor between unilateral and bilateral clefts.

II. LITERATURE REVIEW

II.1. Cleft lip & Palate

Cleft lip with or without cleft palate (CL/P) is a congenital craniofacial anomaly that is defined as an opening in the palate and or lip. Cleft lip and palate is the most common craniofacial congenital anomaly (Seifeldin et al., 2015) and the second most common birth defect in the US (Parker et al., 2010). It has an incidence of 1 in every 940 live births, according to CDC data (Parker et al, 2010). Cleft lip and palate prevalence varies with different races and is reported to be highest in Asians (1 in 500) and lowest in Africans (1 in 2500) (Parada et al., 2012). Cleft lip and palate also has sex variance as it is more prevalent in males than females at a ratio of 2:1 (James et al., 2000)).

II.2. Etiology & risk factors

Regarding etiology, CL/P can be divided into syndromic CL/P which are associated with other malformations and non-syndromic CL/P which are an isolated trait. Syndromic CL/P can be due to single gene transmission, teratogens or environmental factors (Muhammed et al., 2014). On the other hand, non-syndromic CL/P is diagnosed by exclusion and it is multifactorial (Muhammed et al., 2014). It is thought to be caused by an interplay between genetics, environmental factors/teratogens (Dixon et al., 2011; Muray et al., 2002). Genetics accounts for almost two thirds of CL/P with involvement of the IRF-6 gene that has been constantly associated with CL/P (Dixon et al., 2011; Zucchero et al., 2004). Examples for environmental factors are maternal smoking and maternal age <40 (Shi et al., 2008; Herkrath et al., 2012). Potential teratogens include retinoic acid, phenytoin, and valproic acid (Jentink et al., 2010).

II.3. Alveolar Clefts

Cleft lip with or without cleft palate severity ranges from a microform cleft (not obvious externally) to a complete cleft (Figure 1). An alveolar cleft is a cleft in the primary palate located anterior to the incisive foramen. This cleft usually extends from the incisive foramen to the alveolus reaching the lip. Embryologically, primary palate formation occurs during the 4th-7th week of gestation during which the median nasal prominence develops from the frontonasal prominence. Therefore, because of its embryological origin alveolar clefts are always associated with cleft lip but not isolated cleft palate (Bajaj et al., 2003). The most common location for an alveolar cleft is between the lateral incisor and canine, which marks the embryological boundary between the premaxilla and the maxilla proper (Bajaj et al., 2003).

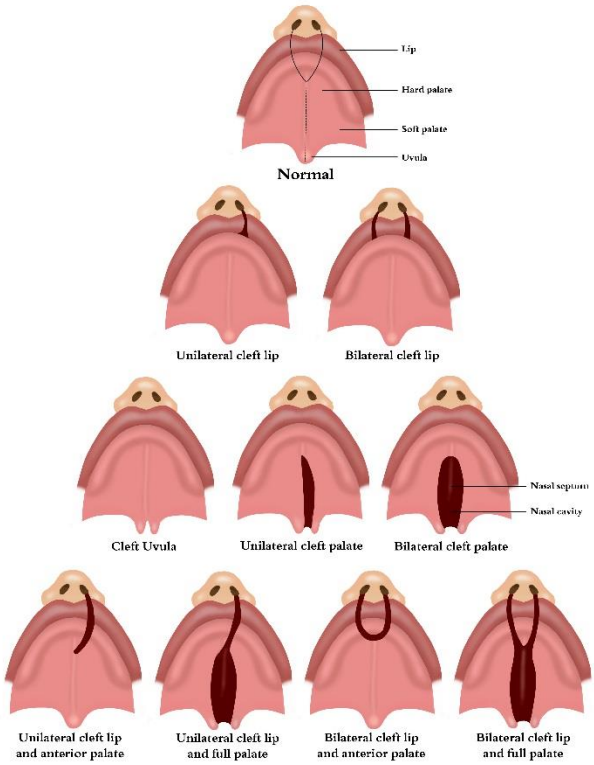

Figure 1. Different types of cleft lip and palate

II.4. Treatment of Alveolar cleft

The rationale behind treatment of alveolar clefts are as follows:

1. Stabilize maxillary alveolus and teeth
2. Support tooth eruption
3. Remove oro-nasal fistulae
4. Improve esthetics
5. Improve speech

Treatment of alveolar cleft may start as early as infancy with pre-surgical infant orthopedics (PSIO), which is divided into two types: fast and slow. An example of a fast PSIO is the Latham protocol while naso-alveolar molding (NAM) is an example of a slow. The objective of PSIO is to bring the two alveolar segments closer together. The fast PSIO utilizes a fixed appliance retained to the alveolus by pins and works actively by traction through elastomeric modules to approximate the segments. On the other hand, slow PSIO maintains the distance between the two maxillary segments while an external source applies the force. Nasoalveolar molding has additional objectives over active PSIO: 1) Molding and approximation of alveolar segments. 2) Repositioning of nasal cartilage. 3) Lengthening of columella.

Regarding surgical treatment of alveolar clefts, surgery plays a vital role in achieving the key objects objectives of treatment of alveolar clefts. However, initial repair of the alveolar cleft is highly controversial (Bajaj et al., 2003). Hopper et al., (2013) advocates for primary gingivoperiosteoplasty (GPP) as a method for initial repair for the alveolar cleft defect. Gingivoperiosteoplasty works on removing the soft tissue barrier from both ends of an alveolar cleft and replaces it with a gingivoperiosteal flap in the form of a soft tissue tunnel designed to facilitate bone conduction in the cleft area. Advantages of GPP include facilitating bone conduction through guided tissue regeneration (GTR) and eliminating the need for bone graft and

donor site morbidity (Hopper et al., 2013). However, critics argue that this method is associated with restriction of midfacial growth and some patients still needs a secondary bone graft later (Kyung et al., 2015).

On the other hand, alveolar bone grafting has been advocated (Daw et al., 2004; Bajaj et al., 2003). It can either be done early (primary graft) or later (after infancy; secondary graft) (Bajaj et al., 2003). Primary bone grafting is performed before 2 years old. Advocates reports that primary bone grafting reduces transverse maxillary deficiency and brings the teeth into better occlusion, thus it minimizes orthodontic treatment (Bajaj et al., 2003). However, it has been reported that primary bone grafting is associated with midfacial growth restriction, poor arch form and less bone formation in the cleft area (Bajaj et al., 2003).

Secondary bone grafting is subdivided into early conventional and late according to age. Early secondary bone grafting is performed between the ages of 2-5 years old, while late secondary is done during the mixed dentition after the eruption of lateral incisor and before the eruption of the permanent canine (Bajaj et al., 2003). According to Kang et al. (2017), late secondary bone grafting provides better stability and enhances facial esthetics through superior bone formation and induction of tooth eruption and nasal support (Figure 2).

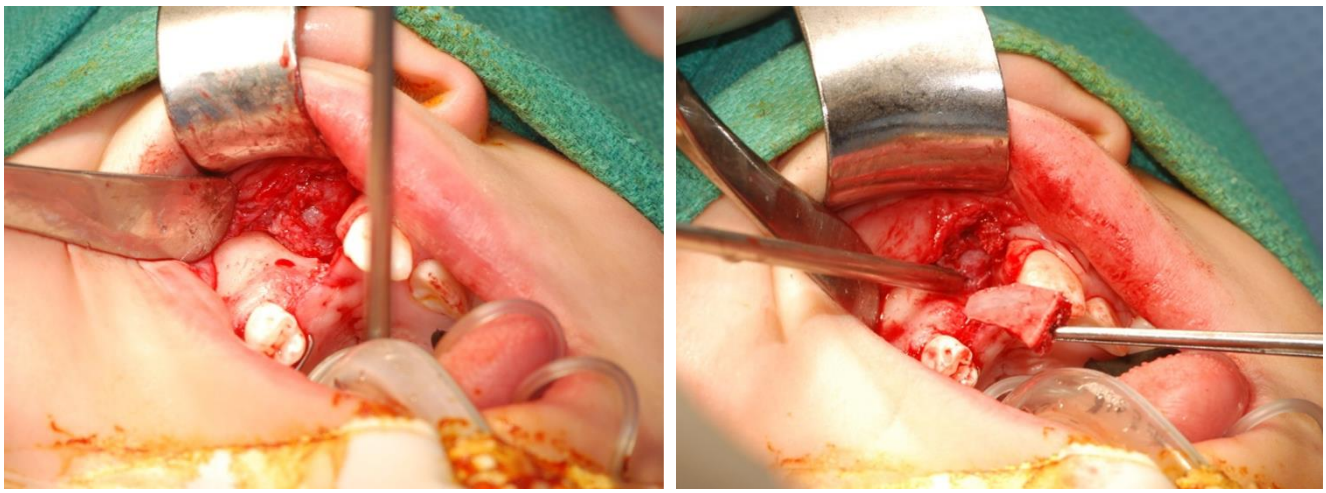

Figure 2. An example of an alveolar cleft repair using an autogenous graft

Regarding grafting materials, both cortical and cancellous bone grafts have been used. Cortical bone grafting relies on vascular ingrowth and works by creeping substitution (Bajaj et al., 2003). In contrast, cancellous bone has higher osteo-induction and osteo-conduction properties and helps in cell transfer and revascularization faster and with better quality than cortical bone (Kang et al., 2017). Although a cancellous bone grafts have been the preferred type, a combined approach has been suggested by some (Precious et al., 2009; Vandeputte et al., 2019). This combined method uses a piece of cortical bone for grafting the nasal floor to separate the nasal mucosa from the cancellous bone graft, arguing that it supports the nasal site and it prevents displacement of the cancellous graft into the nasal cavity (Precious et al., 2009; Vandeputte et al., 2019). Vandeputte et al. (2019) reported that it is a safe technique that does not affect the rate of minor or major complications compared to the use of only a cancellous bone graft. On the other hand, Albrektsson et al. (1980) reported that a cortical graft takes longer to harvest, and it has the potential to a higher risk of graft un-integration and total graft loss.

A cancellous bone graft can be harvested from several sites, for example, the iliac crest, cranium, tibia and ribs. The iliac crest is often the preferred site for its ease of harvest, abundance of cancellous bone and ability to harvest the graft and prepare the cleft site at the same time (Bajaj et al., 2003). The method of harvesting the graft is still also controversial. Sherma et al., (2011) compared the conventional open iliac bone harvest using an osteotomy and a less invasive method using Acumed power-driven trephine system. They reported that the latter showed significantly superior results in term of shorter operative time, less postoperative pain and medication needs, less pain on discharge and shorter hospital stay length (Sherma et al., 2011).

Another aspect to consider in alveolar cleft treatment is orthodontic preparation before the graft (Bajaj et al., 2003). Realignment and widening of the maxillary segments are advocated when needed. Bittermann et al. (2019) has reported that maligned maxillary alveolar segments are associated with higher surgical complications rate. They reported that 42% of patients with displaced maxilla required revision surgery although semi-rigid stabilization with a splint was utilized (Bittermann et al., 2019) (Figure 3).

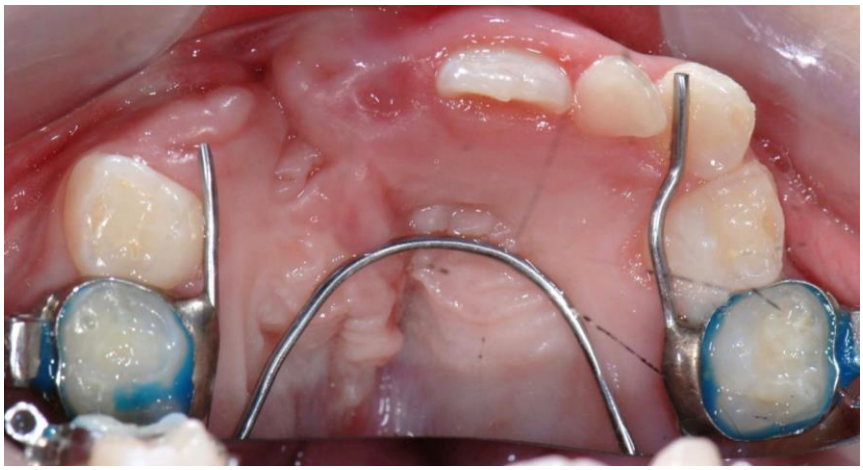

Figure 3. An example of pre-surgical orthodontic treatment for widening of the maxillary segments

Despite the controversy regarding timing and method of alveolar cleft surgical treatment, secondary bone grafting with cancellous bone from the iliac crest is currently considered by most to be the gold standard for treatment of alveolar clefts (Bajaj et al, 2003). Nevertheless, some disadvantages are reported. In 1998, the Clinical Standards Advisory Group (CSAG) assed the radiographic bone level following secondary bone grafting in 157 case and reported a failure rate of 42% (Sandy et al., 1998). Later, Revington et al. (2008) studied 235 grafted sites and reported a failure rate of 24%, with both studies using the modified Kindelan index for radiographic bone assessment. Donor site morbidity is another downside of autogenous bone grafting. Brudnicki et al. (2018) studied donor site morbidity reported that 93% of the patients reported pain equal to or exceeding the recipient site, while 92% reported gait disturbances following surgery. A lower percentage reported an unsightly scar (23%) and iliac contour alteration (40%). They also reported a significant correlation between age and pain, with a higher incidence of pain after the graft surgery in older females (Brudnicki et al., 2018).

II.5. New Developments in Treatment Modalities

Considering the drawbacks of current treatment, new treatment modalities are being investigated. Developments in regenerative medicine offer improved osteoconductive properties, for example, by adding fibrin glue or other materials to an autogenous graft (Berger et al., 2015). Alternatively, enhancing the osteo-inductive properties by using cytokines, such as those of the bone morphogenetic protein (BMP) is one newer potential method for promoting bone growth at the repair site (Berger et al., 2015). Recently, Ferreira et al. (2018) evaluated the use of deproteinized bovine bone (DBB), β-tricalcium phosphate (β-TCP) with autogenous bone from the iliac crest and chin, and reported that the use of DBB, B-TCB with an autogenous graft resulted in less amount of bone graft harvested and consequently less donor site morbidity and hospitalization time (Ferreira et al., 2018).

However, even with these recent developments, the ideal would be to eliminate the need for autogenous bone graft entirely to eliminate donor site morbidity. Ferreira et al.'s (2018) study also revealed that the use of bovine hydroxyapatite as grafting material leads to the formation of bone with less density compared to autogenous graft. On the other hand, Scalzone et al. (2019) reviewed several studies comparing the use of recombinant human bone morphogenetic Protein-2 (rh-BMP2) graft versus autogenous bone graft in maxillary alveolar reconstruction in unilateral cleft lip and palate. The studies they reviewed assessed the graft site using CBCTs six months to a year following grafting. Their meta-analysis found that rh-BMP2 grafts gave similar results in terms of bone height and volume compared to autogenous graft while rh-BMP2 grafts had the advantage of a shorter hospital stay length (Scalzone et al., 2019).

There has also been a trend towards the development of cell-based tissue engineering methods for bone repair and regeneration. In tissue engineering strategies, three elements are of interest: scaffolds, cells and mediators (Berger et al., 2015). Berger et al., (2015) investigated the technical and biological feasibility of using scaffold-based tissue engineering in alveolar cleft osteoplasty. They 3D printed five unilateral cleft lip and palate cases using tricalcium phosphate 4 granulate (TCP) for the scaffold material. After that, they added commercially available human mesenchymal stem cells (hMSCs) to the scaffold and monitored cell survival, proliferation and osteogenic differentiation of hMSCs using scanning electron microscopy (SEM), WST-1 assay and alkaline phosphatase (ALP) assay. In their findings, they reported success of the 3D printing of custom-made scaffolds that are almost identical to the 3D digital model. Moreover, successful seeding of the applied mesenchymal stem cells at %91 was observed. They also noted successful osteogenic differentiation of the scaffold-seeded cells and after 3 weeks of cell proliferation, SEM displayed a pore-border growth of the hMSCs (Berger et al., 2015). Another study took this concept to a more advanced stage and compared the use of dipyridamole and rhBMP-2 in bioceramic scaffolds for treatment of induced alveolar clefts in New Zealand white rabbits. The

authors reported that both materials showed similar mechanical properties in terms of bone regeneration but dipyridamole did not show osteolysis and premature suture fusion as rhBMP-2 (Lopez et al., 2019).

II.6. Alveolar Clefts Typography and Classification

With this new treatment potential, preoperative understanding of the alveolar cleft architecture, size and shape is needed. However, there is still controversy regarding the ideal method to record cleft lip and palate due to the shortcomings and limitations of current classifications (Qiang et al., 2007). Classification systems for clefts have been divided into: embryological and morphological according to Shah et al.(Shah et al., 2011). For embryological classification, the incisive foramen is the dividing point for all. An example of these classification is the one developed by Kernahan and Stark (1958) which is one of the most popular classifications. However, one of its most important shortcomings is that it does not represent the severity of the cleft or degree of involvement. (Shah et al., 2011) There is another recent classification by Qiang et al. (2007) named the LAPAL system, in which it represents both location and extension. It uses Arabic numerals to denote the cleft anatomical location starting with the right lip (L), right alveolus and primary palate (A), secondary palate (P), left alveolus and primary palate (A), and left lip (L) (LAPAL classification). In addition, the extent of clefting is expressed by Arabic numerals from 0 to 4 which represents intact through-complete. This system also accounts for rare atypical forms of clefts by the addition of more numerals. For example, adding numeral 5 represents a median cleft of the upper lip. Furthermore, Qiang et al., (2007) compared between the new numerical classification, the Kernahan (1971) Y classification and the Smith et al. (1998) modification thereof. They reported that both the LAPAL system(the right lip (L), right alveolus and primary palate (A), secondary palate (P), left alveolus and primary palate (A), and left lip (L)) and the Smith were able to represent all cases of cleft while the Kernahan (1971) Y classification was not (Qiang et al., 2007).

Although classifications of clefts might be advancing, current systems still mostly focus on location rather than shape and size. There have been a few studies that investigated and compared clefts defects volume. According to Chou et al., (2019) 3D volumetric assessment of clef site has been reported to reduce donor site morbidity and results in more accurate preparation of bone substitutes in future treatment modalities. The ideal method of volumetric assessment is still a controversy. (Chou et al., 2019) Three studies compared between volumetric measurements of cleft area using 3D printed cleft models versus computer aided engineering virtual 3D models. In addition, one of the studies started with calculating the volume of clefts using a validated algorithm then comparing it to the volume recorded from the other two methods (Kasaven et al., 2016). All studied reported that there was no significant difference between the two methods and that both were accurate in assessing the cleft volume. Although one study reported that virtual 3D Models were the more accurate. The findings of the three studies confirm that both methods can be used in 3D volumetric assessment of alveolar clefts and presurgical planning cleft repair (Chou et al., 2019; Kasaven et al., 2016; Fengzhou et al., 2017). On the other hand, a study by Pa´lha´zi and colleagues (2014) aimed to create a real-size (3D) model template of a bone graft for treatment of alveolar clefts in unilateral cleft lip and palate patients. They constructed 3D digital models of 10 alveolar clefts using cone-beam computed tomography. After that, they used a 3D planning software to create 3D digital models of the alveolar cleft defects(iPlan ENT 3.0, Brainlab, Feldkirchen, Germany) and a 3D printer to print the models. At the end, they concluded that the transfer of the virtual alveolar cleft model into a 3D printed graft template cannot yet be fully achieved; but the 3D visualization of the cleft defect and having a real-size graft template could benefit clinician during alveolar cleft graft surgery (Pa´lha´zi et al., 2014).

In regard to shape, geometric morphometrics has been used before to analyze shape and morphology in cleft lip and palate patients. However, prior work mainly focused on studying the variation of craniofacial morphology and asymmetry in individuals with clefts (e.g., Bugaighis et al., 2010; Toro-Ibacache et al., 2014). Thus, analysis of alveolar clefts shape and its variation using this method have been lacking.

This current study investigated the shape and size of patients with bilateral and unilateral cleft lip and palate defects comparing between them. It was carried out using 3D printing of virtual cleft models following that with geometric morphometrics analysis of the models. This study aimed to further explore the general typography of alveolar clefts and in the same time analyzing and comparing this form of cleft.

III. MATERIALS AND METHODS

III.1. Subjects

Retrospective records of patients with alveolar clefts who presented for secondary grafts at the University of Iowa, College of Dentistry, Department of Orthodontics between 2009 and 2016 for treatment. IRB was approved at the University of Iowa (IRB: 201601711) and an exemption for IRB approval was granted at the University of Illinois at Chicago.

92 subjects were identified, but 32 total subjects remained following the application of the exclusion criteria (see below).

The criteria for inclusion and exclusion in this study were as follows:

III.2. Inclusion Criteria

- Male and female subjects
- Age 5-35 years old at the time of presentation for initial records
- Subjects with Unilateral or bilateral clefts
- Subjects who are undergoing a secondary alveolar graft
- Pre-treatment CBCT radiograph is available

III.3. Exclusion Criteria

- Subjects with successful bridging of bone in the alveolar cleft area
- Subjects with incomplete clefts
- Subjects with other craniofacial anomalies that might affect the cleft area
- Distorted or missing CBCTs

III.4. 3D Model construction

3D Slicer software version 8.1 was used to construct 3D models of alveolar clefts (Pieper et al., 2004). Model creation involved three stages: “painting” and outlining of cleft area; model creation; and model editing (Figure 4).

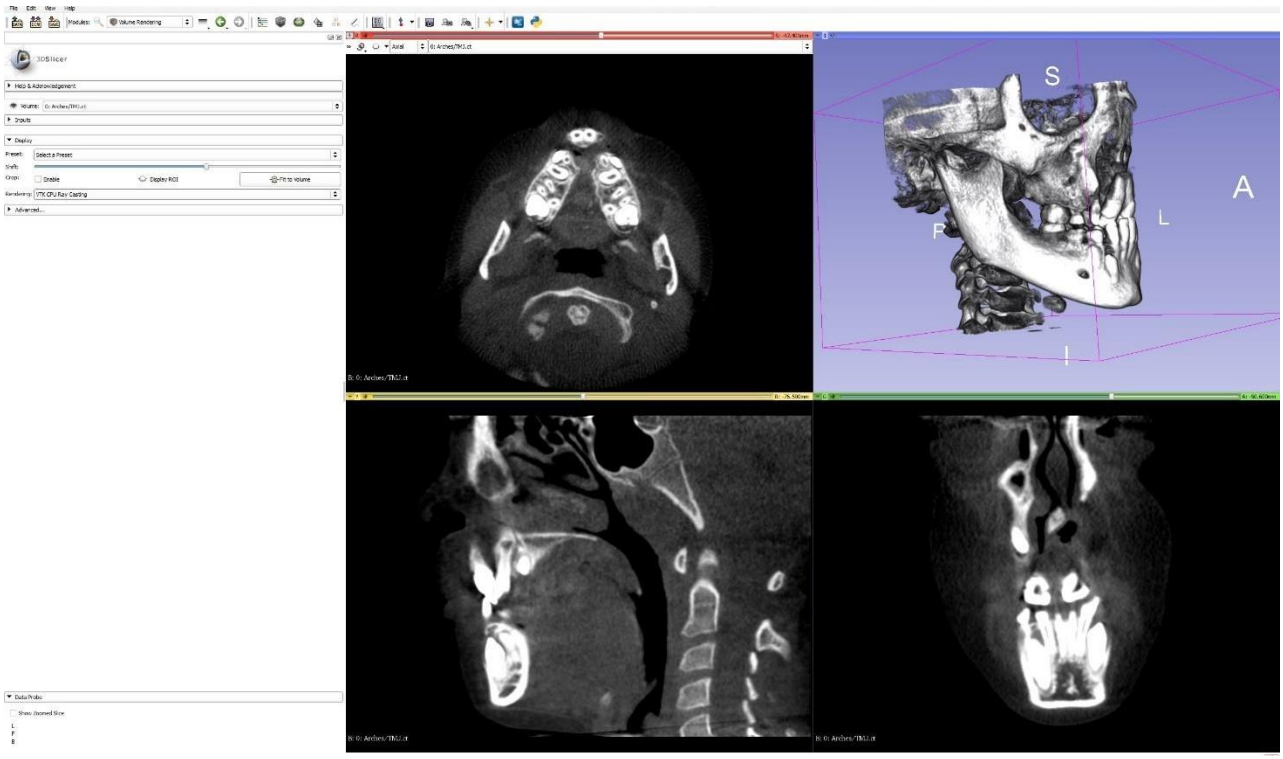

Figure 4. Example of a bilateral alveolar cleft defect opened in 3D slicer software.

In the first stage, “painting” the cleft area, the Editor section of 3D Slicer was used. First a paint threshold for tissue density was identified. Any tissues denser than the selected threshold value will be excluded; in this case, bone and teeth were excluded while soft tissue and air were not (Figure 5). This prevents “painting” on bone and teeth (areas that are “painted” will become a part of the model) and aids in increasing the accuracy of outlining the cleft area. Once the correct threshold was identified, the alveolar cleft was painted through each layer in the axial plane, from anterior to posterior (Figure 6). Care was taken to remain within the boundaries of the alveolar area. After that, the painted area was reviewed through the sagittal view for increased accuracy, to fill in any missed areas and delete any excess.

Figure 5. Paint threshold selection in 3D slicer software.

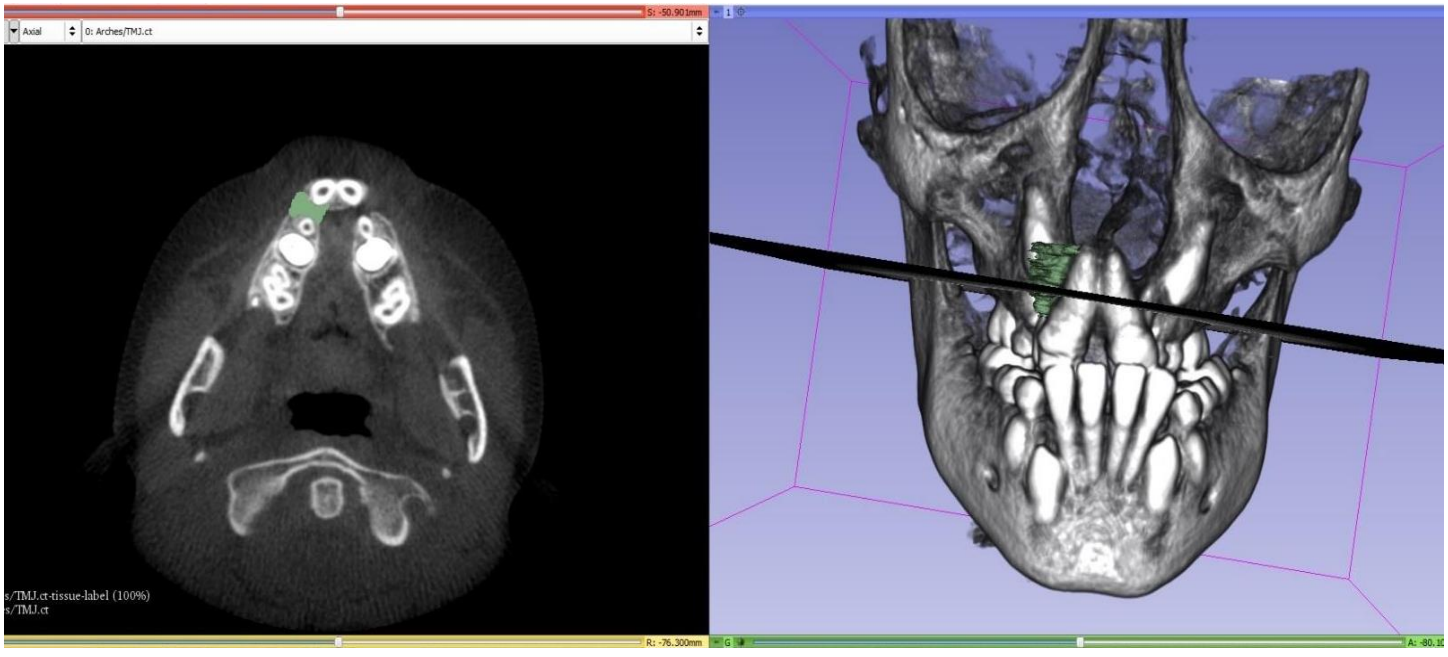

Figure 6. Painting the cleft area in the axial plane in 3D slicer software

In the second stage, model creation was done using the Model Maker tool in 3D Slicer, with setting the parameters of smoothing to 15 and decimating to 0.30. After model creation, model editing was done; it was performed using Geomagic Control software. With the use of different tools, the models were trimmed and smoothed for better representation of the cleft area (Figures 7&8). After model editing the final model was reopened in Slicer together with the CBCT to ensure the accuracy of the final model (the fit to the defect space; see Figures 9&10). Model creation was done by two examiners.

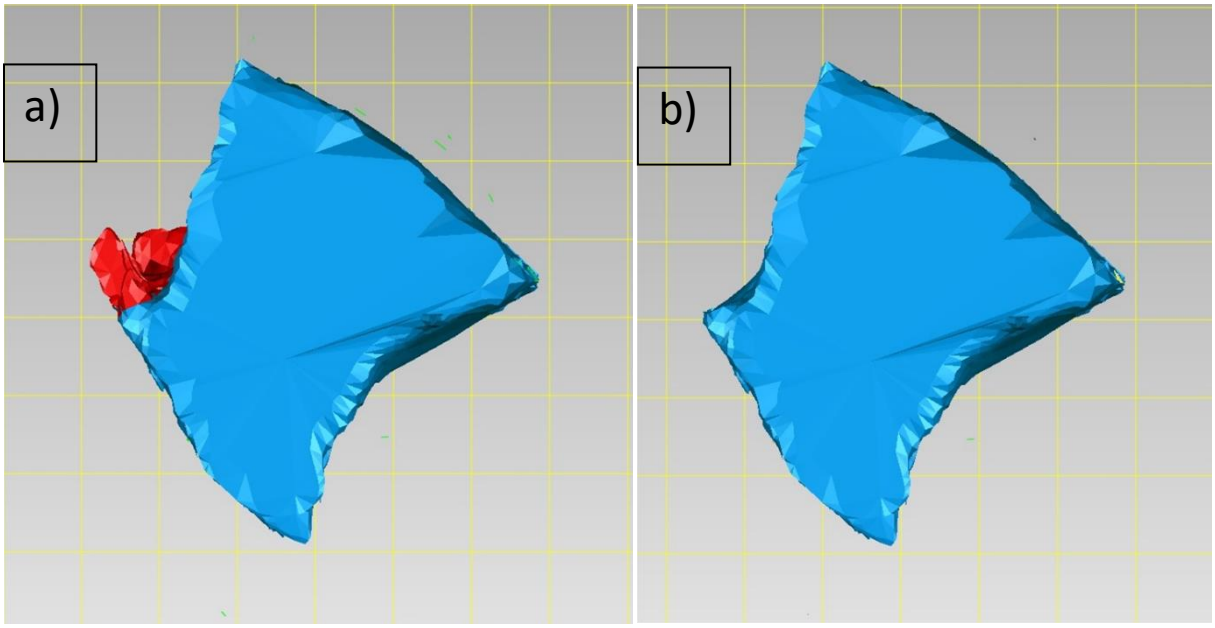

Figure 7. An example of cleaning up artifacts in a 3D cleft model in Geomagic Control software. a) Red marks the area designated for removal are. b) After deletion

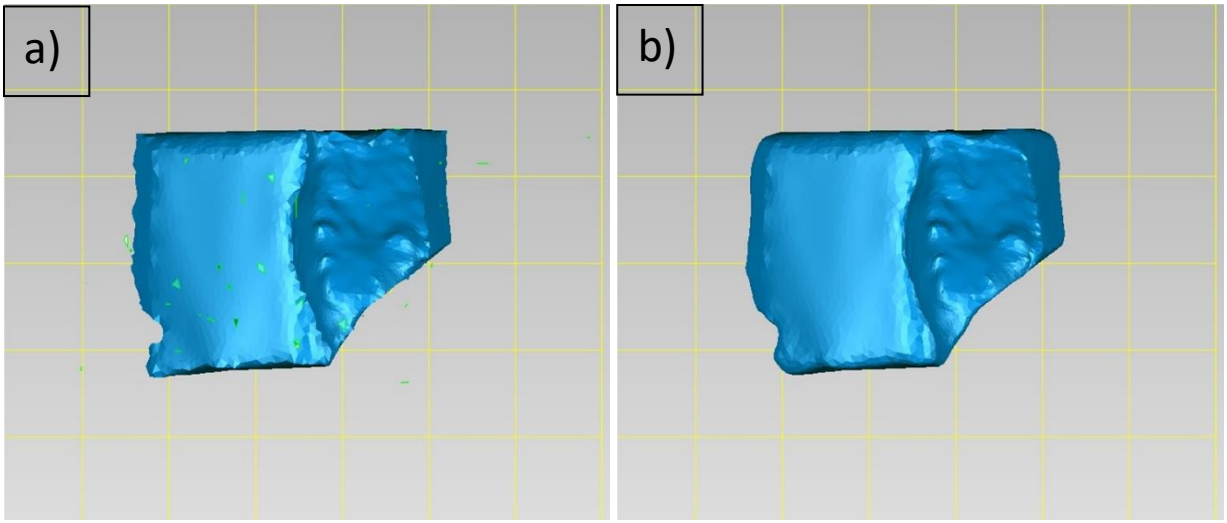

Figure 8. An example of smoothing a 3D cleft model in Geomagic Control software. a) Before smoothing. b) After smoothing

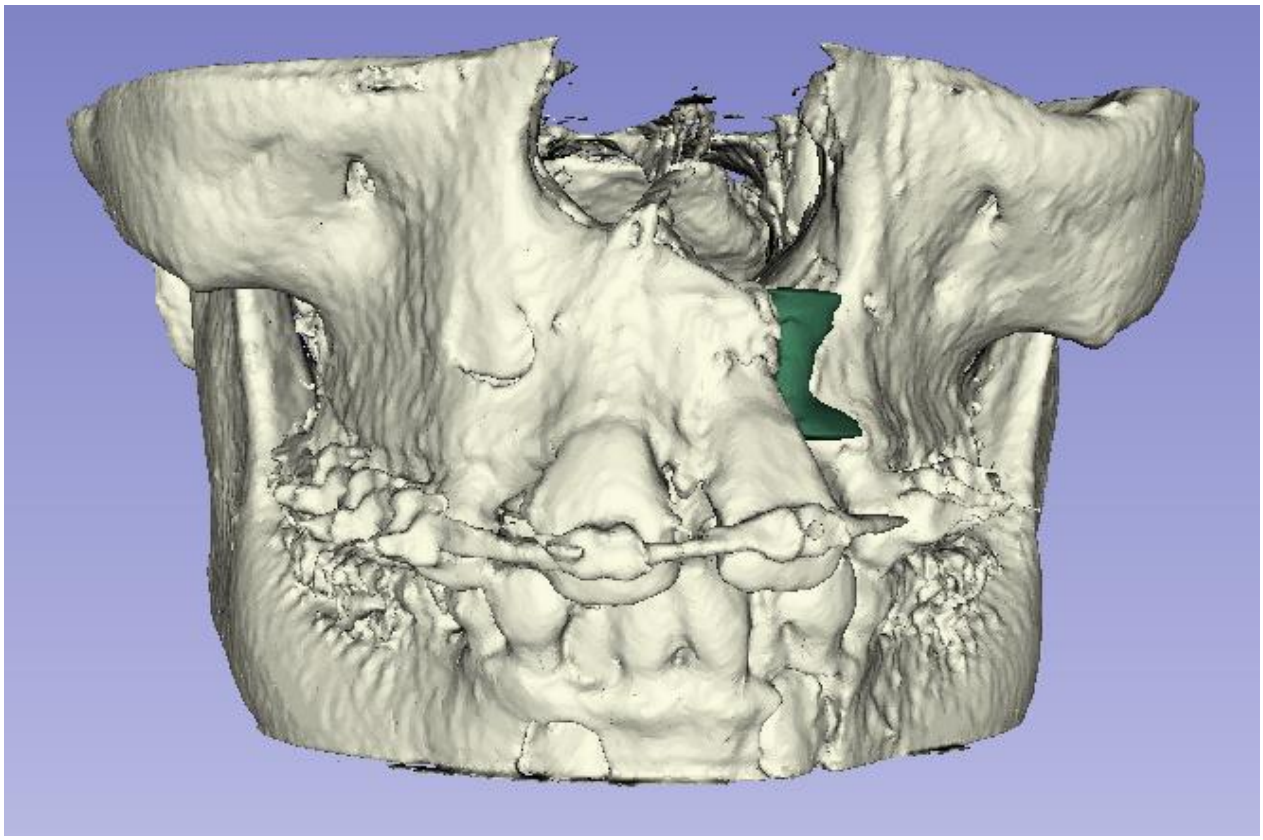

Figure 9. Example of a 3D model and its fit to the defect space.

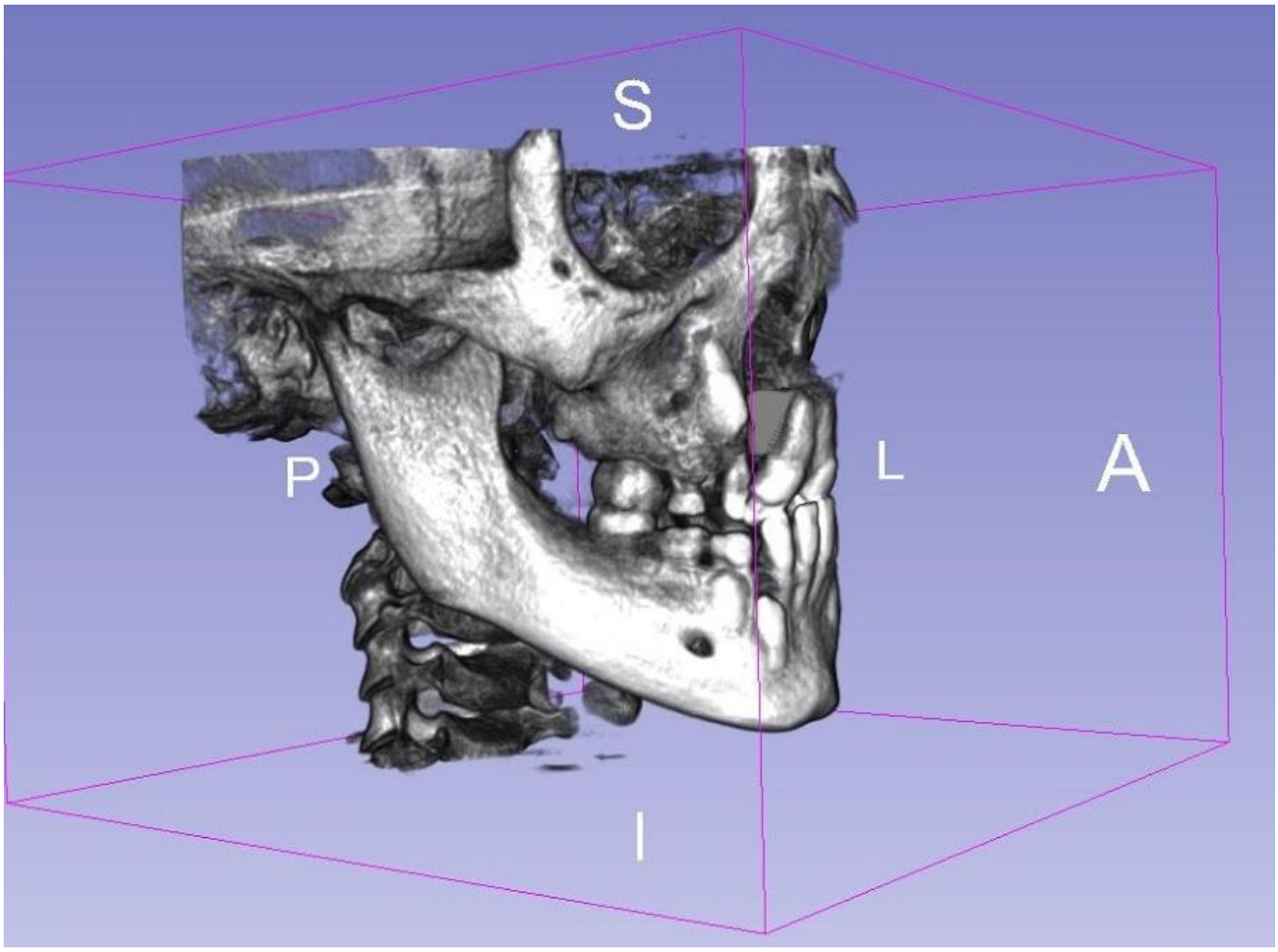

Figure 10. Example of a 3D model and its fit to the defect space.

III.5. Geometric Morphometrics

In the current study, the shape of the models was analyzed using geometric morphometrics (GM). Geometric morphometrics provides both qualitative (visual) and quantitative information on shape variation. In this study, we employ GM to analyze the variation in shapes of alveolar cleft defects.

Shape analysis has been done since ancient times through qualitative description of morphology, but description without quantification makes this data hard to apply. On the other hand, quantitative traditional morphometrics has been used extensively but has various drawbacks. Key drawbacks to traditional morphometrics are the limited ability to visualize shape differences; the fact that linear and angular measurements primarily capture size and shape; and the fact that traditional morphometrics does not typically account for the covariation across measurements (Zelditch et al.., 2012).

The need for a method that quantifies but also provides visualization of shape data is what gave rise to GM. It emphasizes the biological component together with mathematical analysis through the use of a set of landmarks. Geometric Morphometrics provided more precise illustration, allowed for statistical analysis and algebraic description. In addition, it allowed for a more detailed comparison of the differences between complex shapes with the ability to visualize these differences (Zelditch et al., 2012). Shape analysis using Geometric Morphometrics involves four steps: landmark identification; removal of non-shape variation and superimposition; statistical analysis; and graphical presentation (Zelditch et al., 2012).

III.6. Landmark Identification:

Homologous landmarks are defined as distinct anatomical loci that can be found in all organisms in the study (Zelditch et al., 2012). Semilandmarks, on the other hand, are non-discrete points that provide information about curvature. Semilandmarks are mathematically rendered homologous through the act of sliding semilandmark-based Procrustes superimposition. They must therefore be anchored by traditional coordinate landmarks (Zelditch et al., 2012).

III.7. Procrustes Superimposition:

There are several types of superimposition which can be employed; for the sake of this study, Procrustes superimposition only will be mentioned as this is the method we employed and is the most common method used in GM. This superimposition is used to minimize the differences between landmark configurations while maintaining their shape through translation, scaling and rotation.

Procrustes superimposition involves three steps as described by Rohlf and Slice (1990):

1. Centralize the alignment of the landmark at the origin by subtracting the correspondents of the centroid from the correspondents of the landmark.
2. Slide the landmark correspondent to centroid size by dividing the correspondent of the landmark by the centroid size of that alignment.
3. Choose one alignment and arrangement to be the base, After that, rotation of the second configuration for less summed squared distance between homologous landmarks.

III.8. 3D Landmarking

We placed 3D semilandmark grids on all 6 surfaces of each cleft defect model using Landmark Editor (Figure 11). Each border of the grid had 2 landmarks anchoring 3 semilandmarks; thus, total we had 4 landmarks and 21 semilandmarks on each of the 6 surfaces of each model.

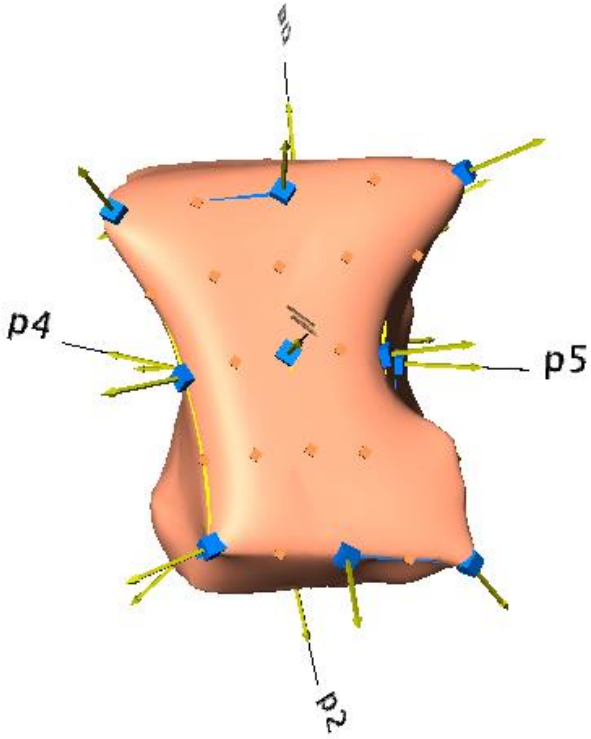

Figure 11. Example of semilandmark grid on anterior surface of 3D cleft model

III.9. Data Analysis

The size (volumetric) data was analyzed using non-parametric tests, because the sample was not normally distributed. To compare volume size, model height, and model width at the nasal floor between unilateral and bilateral clefts, we used the Wilcoxon rank sum tests.

For our GM data, we ran a series of cluster analyses to determine whether there were common 'types' of cleft defect shapes. Firstly, we calculated Procrustes distances between our GPA transformed samples and used a Gaussian finite mixture model fitted by an EM algorithm to determine the ideal number of clusters. We also investigated the Bayesian Information Criterion for our sample. The results of which were used to determine whether any other clustering models might be worth investigating. We then ran a K-means cluster analysis to examine our potential models.

In order to further examine our clustering models, we ran a principal components analysis (PCA) on our Procrustes-transformed landmark data. Scatterplots of the PC's that represented >5% of the overall variation were used to visualize differences between the clusters.

IV. RESULTS

IV.1. Descriptive statistics of Alveolar Defects Size:

In respect to volume, the average volume for alveolar defects was 783.9 mm^3, while the median and standard deviation were 661 mm^3 and 361.1 respectively (Table I).When comparing the volumes of unilateral and bilateral defects, unilateral defects were on average larger (938.4 mm^3) compared to the bilateral defects (658.9 mm^3). Moreover, unilateral defects had also a larger standard deviation than the bilateral defects (Table II & III).

Regarding the height of the alveolar defects, the average height for the whole sample was 12.17 mm with a standard deviation of 2.35 (Table I). In addition, the average height for the unilateral sample was measured at 13.07 mm with a standard deviation of 2.81 (Table II). On the other hand, the average of the bilateral sample was measured shorter at 10.06 mm with a standard deviation of 1.04 (Table III).

As for the width at the nasal floor, the average width for the whole sample was 11.62 mm with a standard deviation of 3.71 (Table I). The average width for the unilateral sample came at 12.35 mm with a standard deviation of 3.60 (Table II). The average of the bilateral sample was also shorter at 9.88 mm with a standard deviation of 2.90 (Table III).

The range of variation between the maximum and the minimum of each of the measurements of alveolar defects is listed in (Table IV).

TABLE I. ALVEOLAR DEFECTS VOLUME OF WHOLE SAMPLE

	Volume	Height	Width at the nasal floor
Average	783.9592	12.17965	11.62219
Median	661.0105	10.515	11.76
Standard Deviation	361.1553	2.350452	3.719364

TABLE II. ALVEOLAR DEFECTS VOLUME OF UNILATERAL SAMPLE

	Volume	Height	Width at the nasal floor
AVE	938.4208	13.07385	12.35673
MED	887.9375	13.065	11.395
SD	370.9547	2.814596	3.60394

TABLE III. ALVEOLAR DEFECTS VOLUME OF BILATERAL SAMPLE

	Volume	Height	Width at the nasal floor
AVE	658.9952	10.06609	9.886
MED	625.744	10.11	8.96
SD	130.478	1.048373	2.906193

TABLE IV. MAX-MIN IN ALVEOLAR DEFECTS SIZE

Bilateral	Volume	Height	Width_at_NF
Max	1011.3	11.68	14.54
Min	493.5	8.517	6.12
Unilateral	Volume	Height	Width_at_NF
MAX	1928.8	17.81	20.12
MIN	283.06	7.3	7.45
Combined Sample	Volume	Height	Width_at_NF
Max	1928.8	17.81	20.12
Min	283.06	7.3	6.12

IV.2. Comparing Unilateral and Bilateral Alveolar Defects Size

The size data was analyzed using Wilcoxon rank sum test (non-parametric tests) since the sample was not normally distributed. When comparing unilateral and bilateral alveolar clefts volume, there was a statistically significant difference between them ($p= 0.015$) In addition, there was a statistically significant difference between unilateral and bilateral alveolar clefts height ($p= 0.0014$). However, the width at the nasal floor comparison was statistically not significant although it was approaching borderline of significance ($p=0.06$)

IV.3. Shape Analysis

A generalized Procrustes analysis was run on the 3D coordinate landmark data, allowing for our semi-landmark grids to slide along their tangents based upon Procrustes distance (Rohlf, 2010). After identifying and removing outliers, we were left with n=30 models. We calculated Procrustes distances between the 30 models and used a Gaussian finite mixture model fitted by an EM algorithm to determine the ideal number of clusters. We identified a 2-cluster model as best fitting the data (Figure 12), yielding 1 larger cluster (n=27) and one smaller cluster (n=3). However, using the Bayesian Information Criterion (BIC), we see a drop-off after 5 components (Figure 13), so an alternative considered here is a 5-cluster model. We then used K-means clustering to examine a 2-cluster and 5-cluster model, respectively.

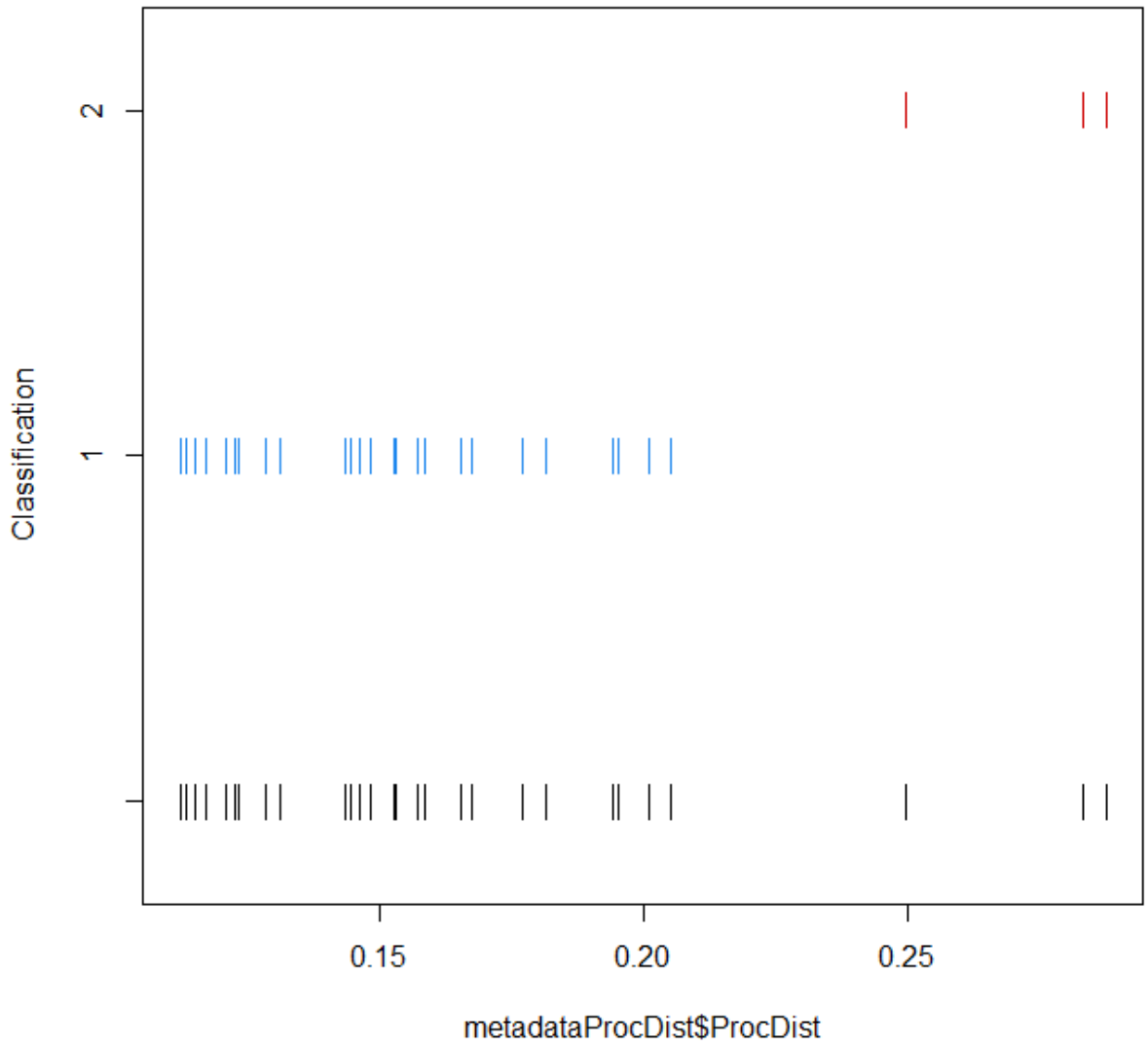

Figure 12. A 2-Cluster model was found to best represent the data.

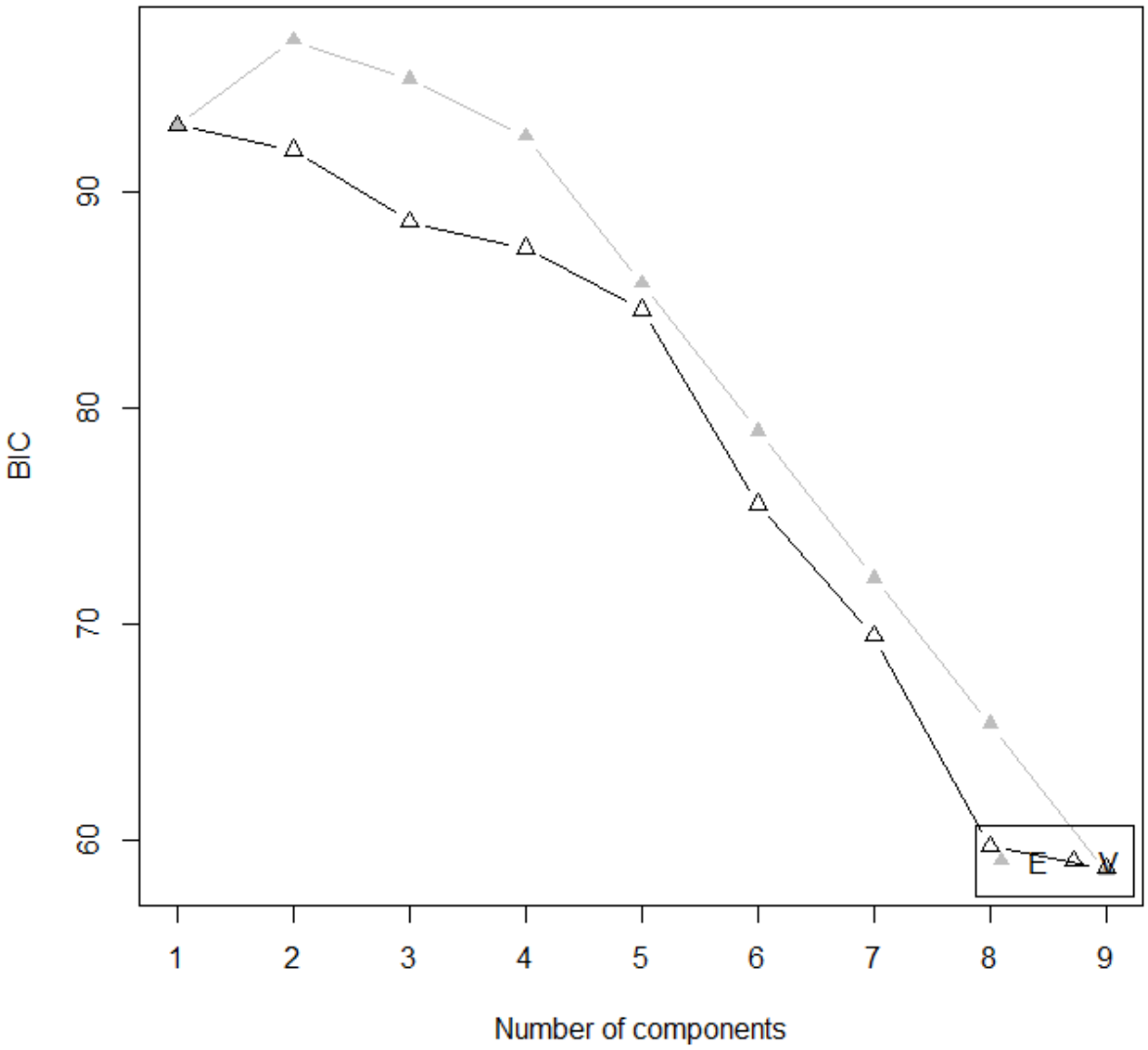

Figure 13. A 5-Cluster model is proposed as an alternative, which may better capture variation that is being grouped into one large group in a 2-Cluster model.

In the 2-Group K-means cluster, Group 1 had an average Procrustes distance of 0.142 while Group 2 had an average of 0.226 (see below for an illustration of examples of models with Procrustes distances which well represent each group; Figure 14). Generally, Cluster 1 models are medio-laterally wider. Average Procrustes distance values for the 5-group K-means cluster are in Table IV (see Fig. 15 for illustrative examples of each group). Cluster 2 models are also generally tall and narrow.

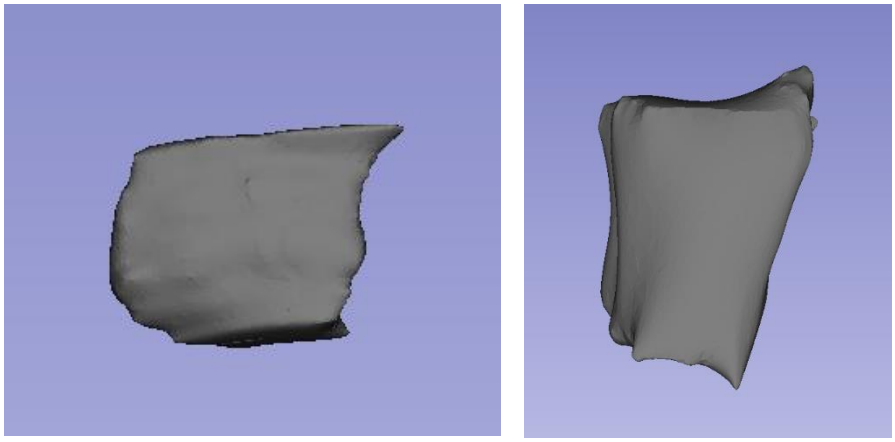

Figure 14. Images depict cleft models representative of the two groups identified by a 2-Cluster Model. Group 1 (left) is represented by models of a variety of shapes, most of which are fairly wide (medio-laterally); Group 2 are models that are medio-laterally wide at the top (superior/nasal floor) surface but much narrower at the bottom (inferior/alveolar) surface. (Images not to scale).

TABLE V. TABLE IV. MEAN PROCRUSTES DISTANCES FOR EACH OF THE FIVE GROUPS IN A 5-GROUP MODEL, AS IDENTIFIED BY K-MEANS CLUSTERING

	n	Mean Procrustes distance
Group 1	4	0.114
Group 2	11	0.153
Group 3	5	0.125
Group 4	3	0.274
Group 5	7	0.193

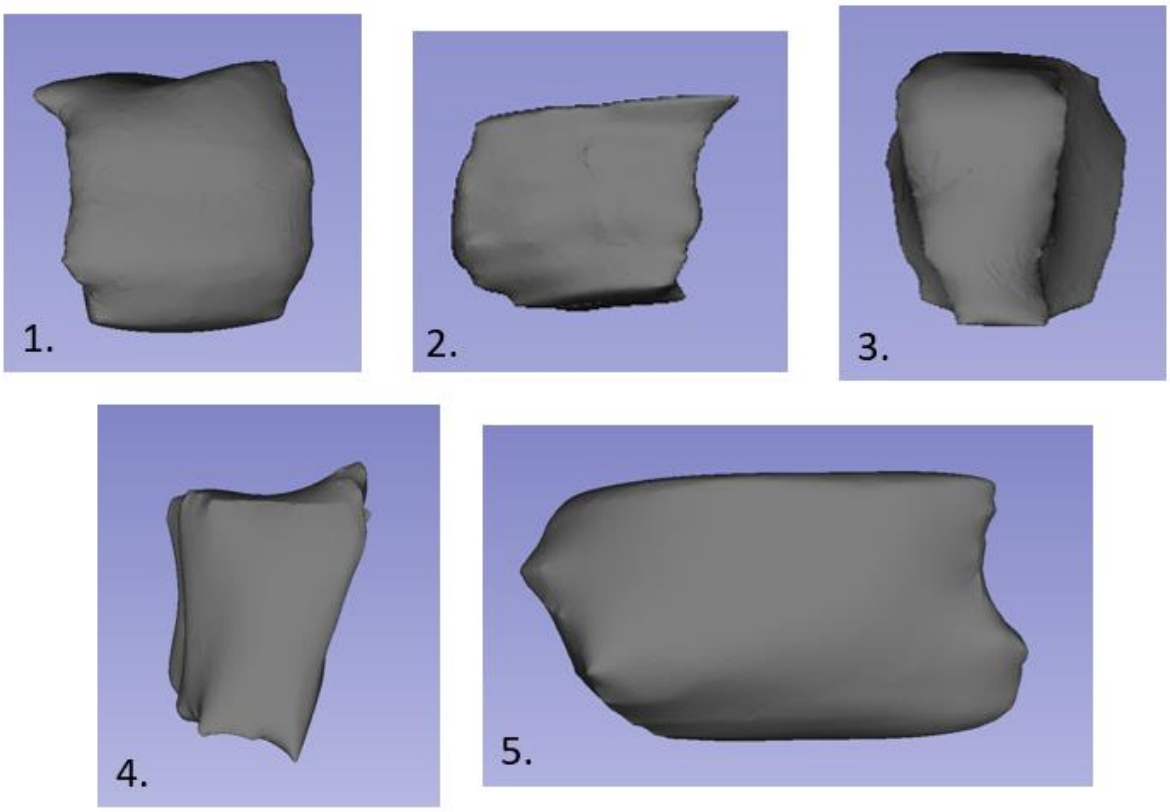

Figure 15. Representative models of the five groups in the 5-Group model from the K-means cluster analysis. The 5-Group model provides are more detailed breakdown of the sample. As can be noted, Group 4 in the 5-Group model overlaps significantly with Group 2 in the 2-Group model, and both are represented by cleft defect models which are tall and narrow. Group 2 (in the 5-Group cluster) was represented by the largest number of individuals and depicts cleft

To further examine the 5-Group model, we ran a principal component analysis (PCA) on our Procrustes-transformed landmark data. The PCA yielded 27 PC's, the first 6 of which each represented >5% of the overall variation. Scatterplots of PC1 x PC2, PC3 x PC4, and PC5 x PC6, using the 5-Group Cluster as a grouping variable, were used to visually examine the relationship between the shapes of the models in the 5 groups (Figs. 16-18). While PC2 very clearly delineates Group 4 (also Group 2 in the 2-Group Cluster) from the other groups, none of the other groupings are particularly distinct.

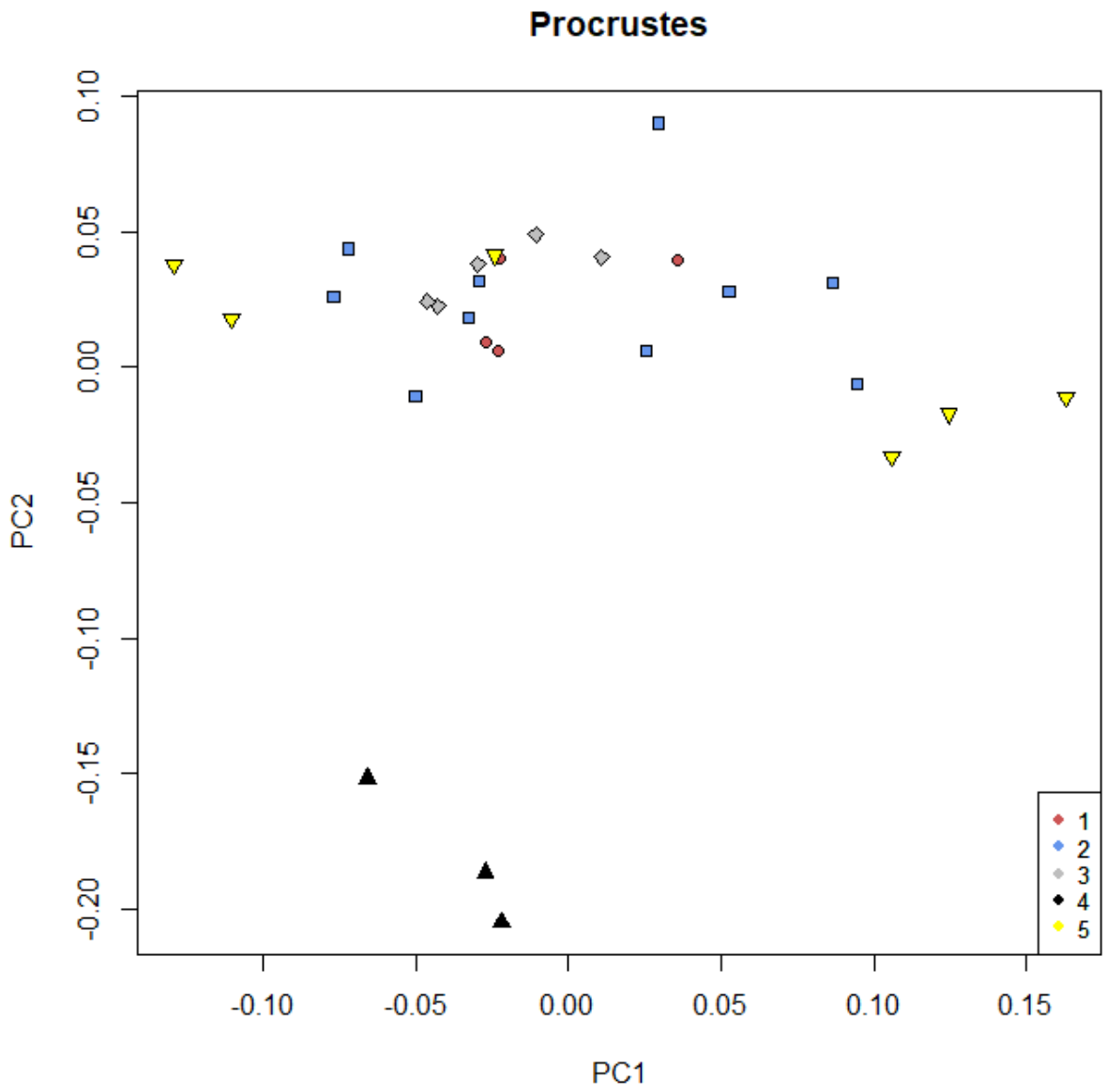

Figure 16. Scatterplot of PC1 and PC2 grouped by the output of the 5-group K-means cluster analysis. PC2 very clearly depicts the difference between group 4 and the other groups.

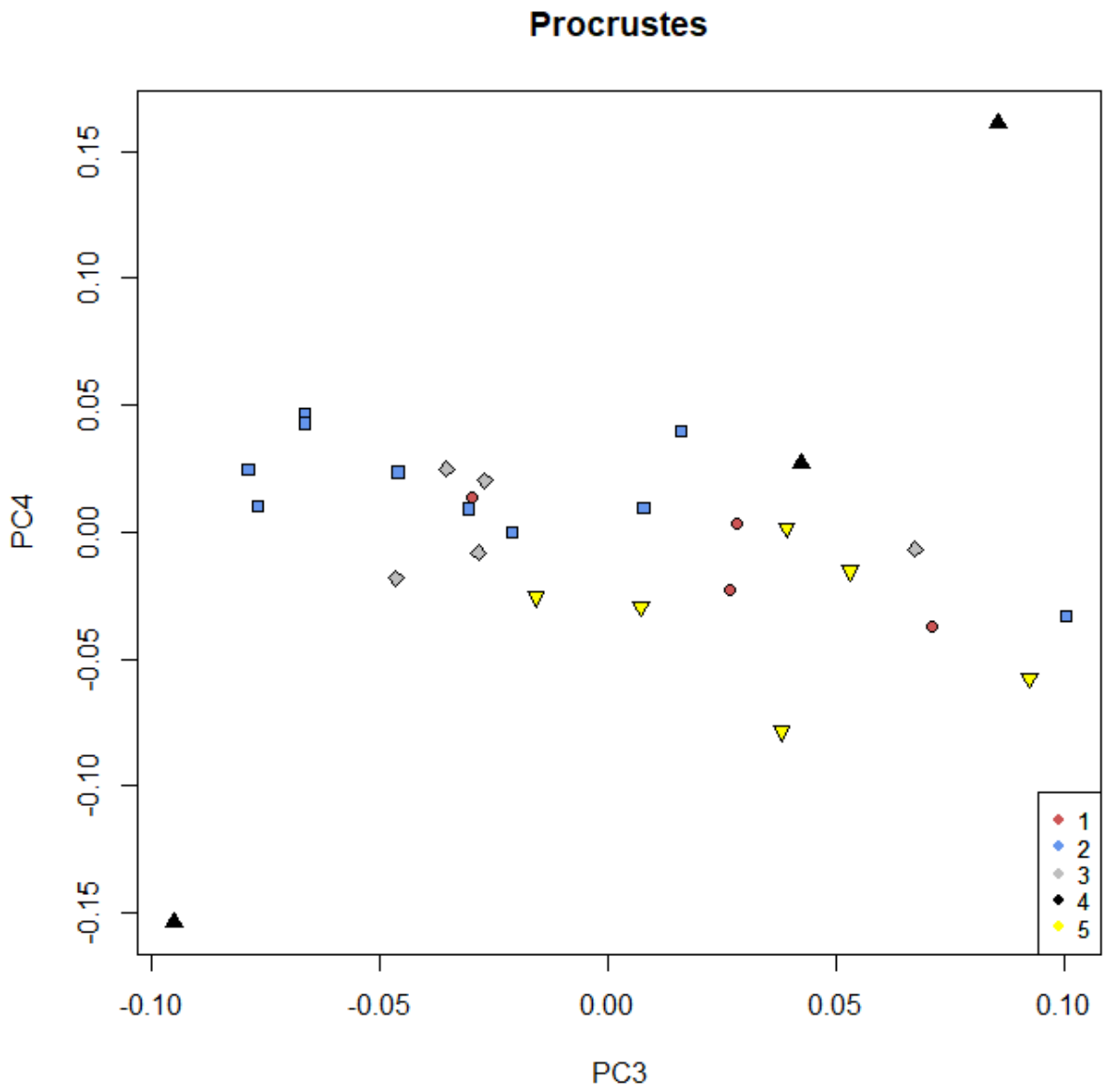

Figure 17. Scatterplot of PC3 and PC4 grouped by the output of the 5-group K-means cluster analysis. Group 5 appears to separate to some degree from the other groups both along PC3 and PC4, while Group 2 represents the opposite pattern (higher PC4 scores, lower PC3 scores)

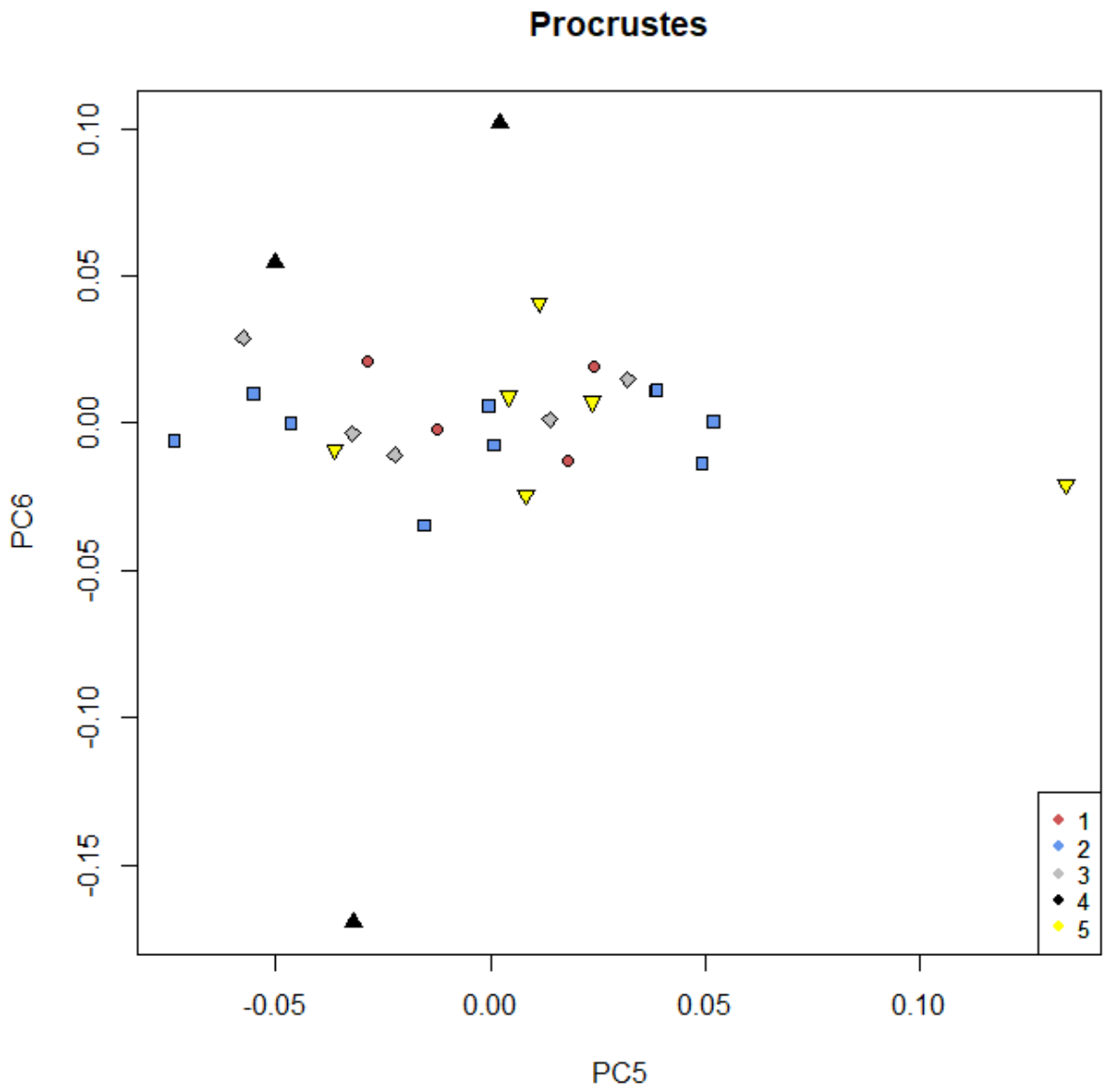

Figure 18. Scatterplot of PC5 and PC6 grouped by the output of the 5-group K-means cluster analysis.

V. DISCUSSION

Cleft lip and palate is the most common craniofacial anomaly and the second most common birth defect in the United States. Although secondary alveolar grating with cancellous bone is considered to be the golden standard, several drawbacks are reported. For further research in future treatment modalities better understanding of the cleft size and morphology is needed. In the current study 3D computer software has been used to analyze the size of unilateral and bilateral alveolar cleft defect. Furthermore, landmark identification and geometrics morphometric has been utilized for shape analysis.

V.1.Shape Analysis Clustering

As can be seen from our shape data, while the data most strongly support a 2-Cluster model, it may be that with a larger sample size, a 5-Cluster model may better represent the true variability in cleft defect shape. The 5-Cluster model described variation in A-P and S-I dimensions (some defects are tall and narrow while others are shorter and wider) as well as overall contour differences (some defects are wedge shaped while many are rectangular or square. Based upon the current results, we would posit that pre-made scaffolds should, at a minimum, represent different square and rectangular dimensions as well as there being scaffolds that are “wedge-shaped” with a wider superior border. Having models of varying dimensions that cover these basic shapes would likely capture a large percentage of cleft defect shapes. Future research is needed to determine ideal increments for the dimensions of these squares, rectangles, and wedges, as well as to estimate what percentage of clefts are each shape.

V.2.Alveolar cleft defects size comparison.

3D computer modeling is a recent method that has been used to measure the volume of the alveolar cleft defect. Two studies have compared the accuracy of this method to estimate the volume of the defects to real scale 3D printing of the defect model (Du et al., 2017; Chou et al., 2019). Both studies' objectives were to measure the volume in order to predict the volume of the bone graft needed for the alveolar cleft repair surgery (Du et al., 2017, Chou et al., 2019). In the current study, the average volume of unilateral alveolar defects was reported at 938.42 mm3. Chou et al. (2019), analyzed the volume of 32 unilateral and bilateral cleft patients using a very similar methodology to the current study except for a different software (SimPlant Pro software package). They reported a similar volume average of unilateral clefts at 1000.09 mm3. Du et al (2017), on the other hand, had a much higher (almost %50) average volume for alveolar cleft defect than both Chou et al and this current study. They reported an average volume at 1470 mm3 when they used a computer-aided engineering (CAE) method to measure the volume for patients with unilateral clefts. However, they mirrored the non-cleft side to obtain a normal morphology of the cleft area, a method cannot be utilized in bilateral clefts (Du et al., 2017); moreover, the protocol for model creation and volume calculation was not specified.

Furthermore, both studies utilized adjacent different densities of CBCT for model production to obtain the measured volumes. Nevertheless, no significant differences or linear relationships were observed between different densities of CBCT (Du et al., 2017; Chou et al., 2019).

V.3.Limitations

The main limitation of this study is the sample size. A larger sample would potentially give more evident results comparing cleft defects size and better clarify any shape clustering patterns. For example, in comparing the width at the nasal floor between unilateral and bilateral alveolar

clefts there was no statistically significant difference, but it was approaching significance (p=0.06). A larger sample size would potentially lead to a more conclusive result.

Another limitation is Sample patients are mixed between patients with failed previous bone grafts attempts and un-operated alveolar clefts which might fail to represent true un-operated cleft defects. However, the current study sample would represent the patient population better being mixed between patients who failed previous bone grafts attempts and those with un-operated alveolar clefts.

V.4.Future Implications

Cell-based tissue engineering methods may give rise to the potential ability to produce pre-made graft materials with different applications. This would simplify alveolar cleft defect repair. In the case that pre-made materials could be standardized, this might also provide access to treatment for individuals living in areas where radiographic diagnostic equipment (for custom scaffolds) is unavailable.

For future research, a larger sample size would be recommended with un-operated cleft defects. Furthermore, the development of a typology of alveolar cleft defects according to size and shape would facilitate future research of scaffolds biomechanics, survivability and comparison between different types to continue the path towards successful 3D printed scaffolds as grafting material for alveolar cleft repair.

VI. CONCLUSION

In conclusion, in our sample, we found unilateral defects measurements to be generally larger than bilateral ones with defect height and volume being statistically significant different. Width of clefts was not statistically significantly different across these groups but was approaching significance. This finding might be a useful consideration for clinicians attempting cleft repair. Our shape cluster analysis identified a 2-cluster model differentiating between clefts that are wide and those that are tall; however, we posit that a larger sample may potentially be better represented with a 5-cluster model which better captures the wide range of shape variation. For example, our 5-cluster model highlighted shape differences between clefts which were square, rectangular, and wedge-shaped. Further research with a larger sample size and un-operated cleft defects is needed to identify any more patterns if present and confirm current size and shape results.

CITED LITERATURE:

Albrektsson T. Repair of bone grafts. A vital microscopic and histological investigation in the rabbit. Scand J Plast Reconstr Surg. 1980;14(1):1-12. doi:10.3109/02844318009105731

Bajaj AK, Wongworawat AA, Punjabi A. Management of Alveolar Clefts. THE JOURNAL OF CRANIOFACIAL SURGERY. 2003;14(6):7.

Berger M, Probst F, Schwartz C, et al. A concept for scaffold-based tissue engineering in alveolar cleft osteoplasty. Journal of Cranio-Maxillofacial Surgery. 2015;43(6):830-836. doi:10.1016/j.jcms.2015.04.023

Bittermann GKP, van Es RJJ, de Ruiter AP, et al. Incidence of complications in secondary alveolar bone grafting of bilateral clefts with premaxillary osteotomy: a retrospective cohort study. Clin Oral Invest. June 2019. doi:10.1007/s00784-019-02977-y

Brudnicki A, Rachwalski M, Wiepszowski Ł, Sawicka E. Secondary alveolar bone grafting in cleft lip and palate: A comparative analysis of donor site morbidity in different age groups. J Craniomaxillofac Surg. 2019;47(1):165-169. doi:10.1016/j.jcms.2018.11.006

Bugaighis I, O'Higgins P, Tiddeman B, Mattick C, Ben Ali O, Hobson R. Three-dimensional geometric morphometrics applied to the study of children with cleft lip and/or palate from the North East of England. Eur J Orthod. 2010;32(5):514-521. doi:10.1093/ejo/cjp140

Chou P-Y, Denadai R, Hallac RR, et al. Comparative Volume Analysis of Alveolar Defects by 3D Simulation. Journal of Clinical Medicine. 2019;8(9):1401. doi:10.3390/jcm8091401

Daw JL, Patel PK. Management of alveolar clefts. Clin Plast Surg. 2004;31(2):303-313. doi:10.1016/S0094-1298(03)00129-9

De Mulder D, Cadenas de Llano-Pérula M, Jacobs R, Verdonck A, Willems G. Three-dimensional radiological evaluation of secondary alveolar bone grafting in cleft lip and palate patients: a systematic review. Dentomaxillofacial Radiology. 2018;48(1):20180047. doi:10.1259/dmfr.20180047

Dixon MJ, Marazita ML, Beaty TH, Murray JC. Cleft lip and palate: understanding genetic and environmental influences. Nat Rev Genet. 2011;12(3):167-178. doi:10.1038/nrg2933

Du F, Li B, Yin N, Cao Y, Wang Y. Volumetric Analysis of Alveolar Bone Defect Using Three-Dimensional-Printed Models Versus Computer-Aided Engineering. Journal of Craniofacial Surgery. 2017;28(2):383-386. doi:10.1097/SCS.0000000000003301

Herkrath APC de Q, Herkrath FJ, Rebelo MAB, Vettore MV. Parental age as a risk factor for non-syndromic oral clefts: a meta-analysis. J Dent. 2012;40(1):3-14. doi:10.1016/j.jdent.2011.10.002

Hopper RA, Al-Mufarrej F. Gingivoperiosteoplasty. Clin Plast Surg. 2014;41(2):233-240. doi:10.1, Murray JC. Cleft lip and palate: understanding genetic and environmental influences. Nat Rev Genet. 2011;12(3):167-178. doi:10.1038/nrg2933016/j.cps.2013.12.006

Jahanbin A, Zarch HH, Irani S, Eslami N, Kermani H. Recombinant Human Bone Morphogenic Protein-2 Combined With Autogenous Bone Graft for Reconstruction of Alveolar Cleft: Journal of Craniofacial Surgery. 2019;30(3):e209-e213. doi:10.1097/SCS.0000000000005160

James WH. Are oral clefts a consequence of maternal hormone imbalance? evidence from the sex ratios of sibs of probands. Teratology. 2000;62(5):342-345. doi:10.1002/1096-9926(200011)62:5<342::AID-TERA8>3.0.CO;2-8

Jentink J, Loane MA, Dolk H, et al. Valproic acid monotherapy in pregnancy and major congenital malformations. N Engl J Med. 2010;362(23):2185-2193. doi:10.1056/NEJMoa0907328

Kang NH. Current Methods for the Treatment of Alveolar Cleft. Arch Plast Surg. 2017;44(3):188-193. doi:10.5999/aps.2017.44.3.188

Kasaven CP, McIntyre GT, Mossey PA. Accuracy of both virtual and printed 3-dimensional models for volumetric measurement of alveolar clefts before grafting with alveolar bone compared with a validated algorithm: a preliminary investigation. British Journal of Oral and Maxillofacial Surgery. 2017;55(1):31-36. doi:10.1016/j.bjoms.2016.08.016

Kyung H, Kang N. Management of Alveolar Cleft. Arch Craniofac Surg. 2015;16(2):49-52. doi:10.7181/acfs.2015.16.2.49

Lopez CD, Coelho PG, Witek L, et al. Regeneration of a Pediatric Alveolar Cleft Model Using Three-Dimensionally Printed Bioceramic Scaffolds and Osteogenic Agents: Comparison of Dipyridamole and rhBMP-2. Plastic and Reconstructive Surgery. 2019;144(2):358-370. doi:10.1097/PRS.0000000000005840

Muhamad A-H, Azzaldeen A, Watted N. CLEFT LIP AND PALATE; A COMPREHENSIVE REVIEW. In: ; 2014.

Murray JC. Gene/environment causes of cleft lip and/or palate. Clin Genet. 2002;61(4):248-256. doi:10.1034/j.1399-0004.2002.610402.x

Pálhazi P, Nemes B, Swennen G, Nagy K. Three-Dimensional Simulation of the Nasoalveolar Cleft Defect. Cleft Palate-Craniofacial Journal. 2014;51(5):593-596. doi:10.1597/13-041

Parada C, Chai Y. Roles of BMP signaling pathway in lip and palate development. Front Oral Biol. 2012;16:60-70. doi:10.1159/000337617

Parker SE, Mai CT, Canfield MA, et al. Updated National Birth Prevalence estimates for selected birth defects in the United States, 2004-2006. Birth Defects Res Part A Clin Mol Teratol. 2010;88(12):1008-1016. doi:10.1002/bdra.20735

Pieper, S., Halle, M., & Kikinis, R. (2004, April). 3D Slicer. In 2004 2nd IEEE international symposium on biomedical imaging: nano to macro (IEEE Cat No. 04EX821) (pp. 632-635). IEEE

Precious DS. A New Reliable Method for Alveolar Bone Grafting at About 6 Years of Age. Journal of Oral and Maxillofacial Surgery. 2009;67(10):2045-2053. doi:10.1016/j.joms.2009.04.102

Qiang Liu, Ming-Liang Yang, Zeng-Jian Li, et al. A Simple and Precise Classification for Cleft Lip and Palate: A Five-Digit Numerical Recording System. Cleft Palate-Craniofacial Journal. 2007;44(5):465-468. doi:10.1597/06-140.1

Revington PJ, McNamara C, Mukarram S, Perera E, Shah HV, Deacon SA. Alveolar bone grafting: results of a national outcome study. Ann R Coll Surg Engl. 2010;92(8):643-646. doi:10.1308/003588410X12699663904790

Sandy J, Williams A, Mildinhall S, et al. The Clinical Standards Advisory Group (CSAG) Cleft Lip and Palate Study. Br J Orthod. 1998;25(1):21-30. doi:10.1093/ortho/25.1.21

Santiago PE, Schuster LA, Levy-Bercowski D. Management of the alveolar cleft. Clin Plast Surg. 2014;41(2):219-232. doi:10.1016/j.cps.2014.01.001

Scalzone A, Flores-Mir C, Carozza D, d'Apuzzo F, Grassia V, Perillo L. Secondary alveolar bone grafting using autologous versus alloplastic material in the treatment of cleft lip and palate patients: systematic review and meta-analysis. Prog Orthod. 2019;20(1):6. doi:10.1186/s40510-018-0252-y

Seifeldin SA. Is alveolar cleft reconstruction still controversial? (Review of literature). The Saudi Dental Journal. 2016;28(1):3. doi:10.1016/j.sdentj.2015.01.006

Shah SNM, Khalid M, Khan MS, Begum S. A REVIEW OF CLASSIFICATION SYSTEMS FOR CLEFT LIP AND PALATE PATIENTS- I. MORPHOLOGICAL CLASSIFICATIONS. In: ; 2011.

Sharma S, Schneider LF, Barr J, et al. Comparison of minimally invasive versus conventional open harvesting techniques for iliac bone graft in secondary alveolar cleft patients. Plast Reconstr Surg. 2011;128(2):485-491. doi:10.1097/PRS.0b013e31821b6336

Shi M, Wehby GL, Murray JC. Review on genetic variants and maternal smoking in the etiology of oral clefts and other birth defects. Birth Defects Res C Embryo Today. 2008;84(1):16-29. doi:10.1002/bdrc.20117

Shkoukani MA, Chen M, Vong A. Cleft Lip – A Comprehensive Review. Front Pediatr. 2013;1. doi:10.3389/fped.2013.00053

Silva Gomes Ferreira PH, De Oliveira D, Duailibe De Deus CB, Okamoto R. Evaluation of the Different Biomaterials Used in Alveolar Cleft Defects in Children. Ann Maxillofac Surg. 2018;8(2):315-319. doi:10.4103/ams.ams_140_17

Tettamanti L, Avantaggiato A, Nardone M, Silvestre-Rangil J, Tagliabue A. Cleft palate only: current concepts. Oral Implantol (Rome). 2017;10(1):45-52. doi:10.11138/orl/2017.10.1.045

Toro-Ibacache V, Cortés Araya J, Díaz Muñoz A, Manríquez Soto G. Morphologic variability of nonsyndromic operated patients affected by cleft lip and palate: A geometric morphometric study. American Journal of Orthodontics and Dentofacial Orthopedics. 2014;146(3):346-354. doi:10.1016/j.ajodo.2014.06.002

Vandeputte T, Bigorre M, Tramini P, Captier G. Comparison between combined cortical and cancellous bone graft and cancellous bone graft in alveolar cleft: Retrospective study of complications during the first six months post-surgery. Journal of Cranio-Maxillofacial Surgery. November 2019. doi:10.1016/j.jcms.2019.11.013

Zelditch ML, Swiderski DL, Sheet HD and Flink WL: Geometric Morphometrics for Biologists: A primer. Academic Press, 2012

Zucchero TM, Cooper ME, Maher BS, et al. Interferon regulatory factor 6 (IRF6) gene variants and the risk of isolated cleft lip or palate. N Engl J Med. 2004;351(8):769-780. doi:10.1056/NEJMoa032909

VITA

Name:	Nora Mohammed Bakhsh
Education:	B.D.S., King Abdul-Aziz University, Jeddah, Saudi Arabia, 2012
	M.S., Oral Sciences, University of Illinois at Chicago, Chicago, Illinois, 2020
Professional Membership:	American Association of Orthodontics